SOLAR SAIL FORCE MODELING FOR SPINNING SOLAR SAIL USING THE RADIOMETRIC TRACKING DATA

Tomohiro Yamaguchi (1), Hitoshi Ikeda (2), Yuya Mimasu (3), Yuichi Tsuda (4), Hitoshi Takeuchi (5) and Makoto Yoshikawa (6)

(1) The Graduate University for Advanced Studies, 3-1-1 Yoshinodai, Chuo-ku, Sagamihara, Kanagawa 252-5210, Japan, yamaguchi.tomohiro@jaxa.jp

(2)(4)(5)(6) Japan Aerospace Exploration Agency, 3-1-1 Yoshinodai, Chuo-ku, Sagamihara, Kanagawa 252-5210, Japan

(3) Kyushu University, Nishi-ku, Fukuoka 819-0395, Japan

Abstract: *This paper investigates the solar sail force modeling of the IKAROS spacecraft using radiometric tracking data. The solar sail force model is one of the key parameter for the practical solar sail mission because the model impacts the overall trajectory design. Since the solar sail force model may have a large uncertainty due to the solar sail deployment and its optical properties, there is a difficulty to configure the model before the launch. This study concentrates on the estimation of solar sail force model for spinning type solar sail with post-launch information. The estimated solar sail acceleration is evaluated with overlap comparison between several tracking conditions.*

Keywords: *Solar sail, Orbit determination, Navigation, Spacecraft modeling.*

1. Introduction

Solar sail is the one of the future technology could expand the deep space explorations, because solar sail have a capability to receive solar photon momentum and obtain acceleration without fuel. Many innovative applications are investigated using solar sails to for space explorations, for instance Mercury, asteroids and outer solar systems [1-3]. Therefore, many space organizations make efforts to realize the technique. For instance, Cosmos 1 project were funded by Planetary Society and try to demonstrate the solar sail technology on the Earth rotating orbit [4]. The 600 m^2 mylar sail was planed to launch by a converted missile, however the launch was failed and also the spacecraft failed to reach the orbit.

Japan Aerospace Exploration Agency (JAXA) is planning “solar power sail”, which is a hybrid system using ion-propulsion engines and solar sail. JAXA is now studying two missions to demonstrate solar power sail. One is small-size solar sail demonstration spacecraft IKAROS (Interplanetary Kite-craft Accelerated by Radiation Of the Sun), which has 14 m x 14 m solar sail with solar cells on the membrane. The minimum success criteria of this spacecraft are the demonstration of the solar sail deployment system and power supply from the thin-film solar cell. The full success criteria of the spacecraft are acceleration and navigation using the solar sail in the interplanetary trajectory. Another spacecraft is the medium-sized solar power sail, which has ion propulsion system with solar sail of diameter 50 m. This spacecraft is planning the launch at mid-2010s and its destinations are the Jupiter and the Trojan asteroids.

IKAROS was launched together with JAXA’s Venus climate orbiter Akatsuki on May 21, 2010. After the separation from H2A launch vehicle, the solar sail was successfully deployed on June 9, 2010, and now it is cruising with solar sail acceleration in an interplanetary space [5]. The spacecraft wet mass is 307 kg including the square-shaped solar sail of 16 kg. The solar sail was deployed and kept the shape by centrifugal force of the spacecraft spinning. Thus it does not have any rigid structure to support the extension of the sail, enabling to achieve very light and simple sail support mechanism. The deployment process was measured and recorded by several onboard equipments, such as cameras, attitude sensors and some surface sensor on the sail. Figure 1 is the picture taken by the separation camera ejected from the IKAROS. It also succeeded to change the attitude using its reflectivity control devices equipped on the edge of the solar sail. The spacecraft continue its flight and it approached Venus on December 8, 2010, one day after the Akatsuki's Venus orbit insertion maneuver. This delay is the consequence of the solar sailing and Fig. 2 illustrates the Venus approaching trajectory of IKAROS. During the interplanetary flight, JAXA ground station collected the radiometric data not only for the tracking, but also for the investigation of the solar sail dynamics.

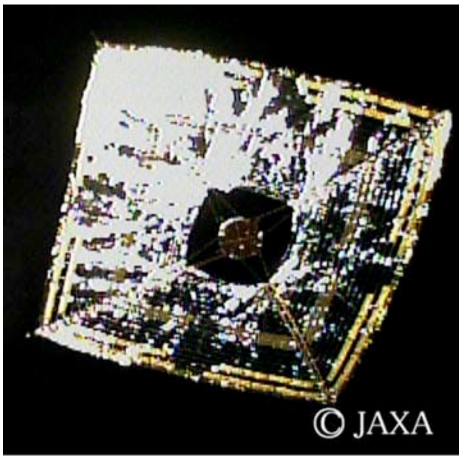

Figure 1. IKAROS image taken by the deployable camera on June 14, 2010

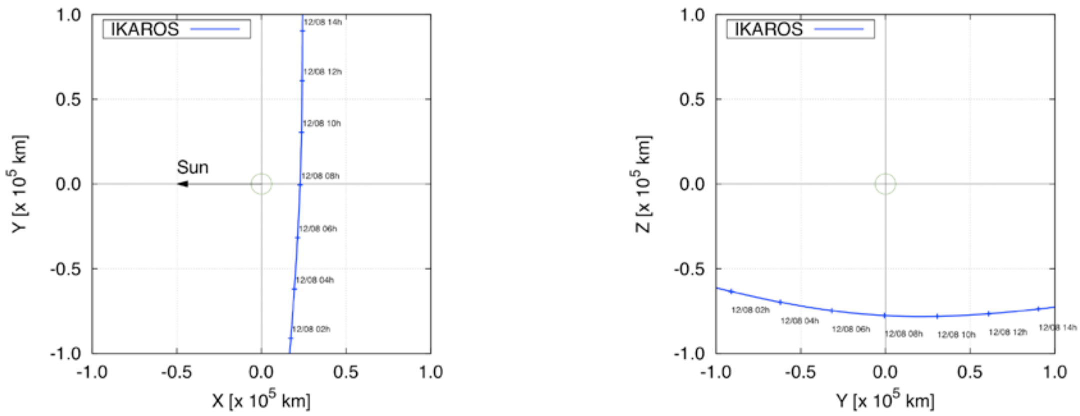

Figure 2. Venus approaching trajectory of IKAROS spacecraft on December 8, 2010 (Venus center, Sun-Venus fixed rotating frame)

In this paper, the solar sail modeling for the IKAROS spacecraft is investigated. First, two solar sail model are introduced in section 2. One is a conventional solar sail model assuming the sail as a single plate and another is the analytical model considering the deformation of the flexible solar sail. Next the covariance analysis for IKAROS solar sail modeling is investigated in section 3. In this simulation, the observability of the solar sail model estimation is mainly discussed. The flight results using the solar sail model are described in section 4. The solar sail model parameters are estimated and evaluated using the actual tracking data. Finally, the conclusions are given in section 5.

2. Solar sail model estimation

This section introduces two solar sail force model for IKAROS spacecraft. Solar sail force estimation is a parameter estimation of solar sail force model. Since the observability of the parameters varies due to the geometry of the spacecraft, the Earth, the Sun and the spacecraft attitude, two models are prepared for solar sail acceleration. The single plane solar sail model is a conventional solar radiation pressure (SRP) model used for many spacecraft and the other is a spinning solar sail model which consider the deformation of the sail.

2.1 Single plane solar sail model

The single plane solar sail model is implemented to estimate SRP acceleration for short tracking arcs. This model assumes a solar sail as a plane composed by a unique material. The acceleration is modeled as following equation, considering absorbing and reflecting component of SRP [6].

$$F = -P(r_S)A\cos\alpha\left\{a_1\hat{r}_S + (2a_3\cos\alpha + a_2)\hat{n}\right\} \tag{1}$$

where $P(r_S)$ is the solar radiation pressure at sun-spacecraft distance r_S, A is the sail's area. $\hat{n}$ is the normal vector of the solar sail and $\hat{r}_S$ is the sun insertion vector, α is called as solar cone angle and calculated by $\cos\alpha = \hat{n}^T\hat{r}_S$, and those vectors are described in Fig. 3. The variable a_1, a_2, a_3 are the optical parameter of the sail surface and they are defined as follows;

$$\begin{aligned} a_1 &= 1 - \rho s \\ a_2 &= B_f(1-s)\rho + (1-\rho)\frac{\varepsilon_f B_f - \varepsilon_b B_b}{\varepsilon_f + \varepsilon_b} \\ a_3 &= \rho s \end{aligned} \tag{2}$$

where B_f, B_b are the sail front and back surface Lambertian coefficients, ε_f, ε_b are the sail front and back surface emissivity, ρ is the sum of the reflectivity, s is the fraction of specular reflection.

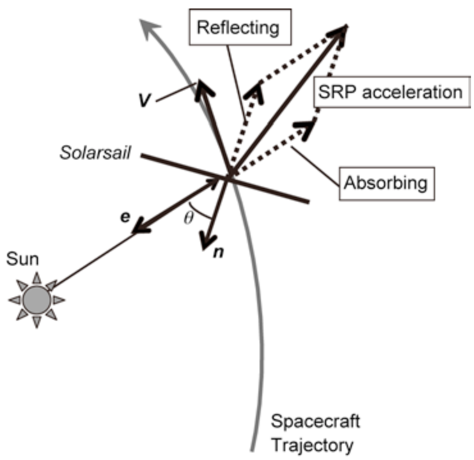

Figure 3. Single plane solar sail model

The spacecraft bass area is neglected assuming the solar sail area is large enough to ignore the area of the spacecraft bass system. In this model, spacecraft area, specular and diffusive reflectivity can be estimated parameter, because those parameters may have large uncertainty due to the deployment or degradation.

2.2 Spinning solar sail model

Since the IKAROS spacecraft has a large flexible membrane, it is important to take into account the effect of the solar sail deformation. In this study, we concentrate on the solar sail force model of the spinning solar sail model which has a outer plane deformation as a function of the distance from the spin axis. The arbitrary outer plane deformation z could be expressed as a function of the distance from axis r as follows:

$$z = f(r) \tag{1}$$

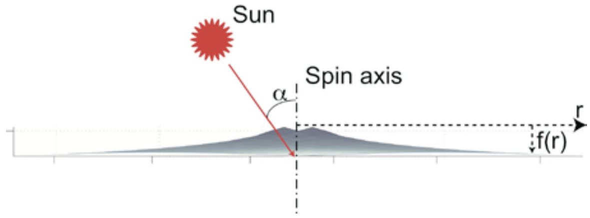

Figure. 4 Deformation of a flexible membrane

Using cylindrical polar coordinates (*(r, φ, z)*, Z axis is parallel to the spin axis), the normal vector of the solar sail elements $\hat{n}$ could define as

$$\hat{n} = \frac{1}{\sqrt{1+f_r}}\begin{pmatrix} f_r\cos\phi \\ f_r\sin\phi \\ 1 \end{pmatrix} \tag{3}$$

where f_r is the partial derivative of outer plane deformation $f(r)$ with respect to the radius r. The solar sail force act on the solar sail element dF is the sum of absorption dF_a, emission and diffusive deflection dF_{d+e} and specular reflection dF_s of the solar radiation pressure. The each force is described as follows;

$$dF_a = P(r_S)a_1(\hat{n}\cdot -\hat{r}_S)\hat{r}_S dA \tag{4}$$

$$dF_{d+e} = P(r_S)a_2(\hat{n}\cdot -\hat{r}_S)(-\hat{n})dA \tag{5}$$

$$dF_s = P(r_S)a_3(\hat{n}\cdot -\hat{r}_S)^2(-\hat{n})dA \tag{6}$$

where $\hat{r}_S$ is the sun insertion vector. Using the solar cone angle α, the components of the sun insertion vector is given in spacecraft fixed frame (X_S, Y_S, Z_S) as $\hat{r}_S = \begin{pmatrix}\sin\alpha & 0 & -\cos\alpha\end{pmatrix}$. Z_S axis is along the spin axis of the solar sail and Y_S axis is defined by $\hat{n}\times\hat{r}_S$. Then, the total force acting on the deformed solar sail is given by

$$\begin{aligned} F_{SRP} &= \int dF_a + dF_{d+e} + dF_s \\ &= P(r_S)\begin{pmatrix} C_1\cos\alpha + C_2\sin\alpha + 4C_4\sin\alpha\cos\alpha \\ 0 \\ -C_1\cos^2\alpha - C_3\cos\alpha - 2C_4\sin^2\alpha - 2C_5\cos^2\alpha \end{pmatrix} \end{aligned} \tag{7}$$

where C_n (n = 1~5) is defined as follows;

$$C_1 = a_1 2\pi\int r dr \tag{8}$$

$$C_2 = a_2\pi\int\frac{rf_r}{\sqrt{1+f_r^2}}dr \tag{9}$$

$$C_3 = a_2 2\pi \int \frac{r}{\sqrt{1+f_r^2}} dr \tag{10}$$

$$C_4 = a_3 \pi \int \frac{r f_r^2}{1+f_r^2} dr \tag{11}$$

$$C_5 = a_3 2\pi \int \frac{r}{1+f_r^2} dr \tag{12}$$

Note that the coefficients are determined independent from the attitude. The coefficient C_1 describes the absorbing effect, C_2, C_3 describes the emission and diffusive reflection, C_4, C_5 describes the specular reflection. The interesting result of this formulation is that the Y_S component of solar sail force is always zero for the spinning solar sail. In case of flat sail model, f_r becomes zero, then the parameters reduce to three (C_1, C_3, C_5) This approach is similar to the Generalized Sail Model introduced by Rios-Reyes[7], though this is specialized for spinning solar sail. In the estimation, the parameter is normalized by the sail's area and described as $\overline{C}_n \ (n = 1 \sim 5)$.

3. Covariance Analysis of Solar Sail Force Estimation

The covariance analysis is provided to understand the ability to estimate the solar sail model parameter. The covariance analysis is performed using pseudo-tracking data. The observable is assumed as X/X 2-way Doppler and range with Usuda 64 m deep space antenna of JAXA. A set of tracking data is generated by 3 days observation without any maneuvers. 5 hours operation per day is assumed and 5 hours Doppler and an hour range measurements are obtained in the operation. A set of tracking data is obtained every 2 weeks for this research. The 1 σ observable accuracy is assumed 0.5 mm/s and 10 m for Doppler and range observable, respectively. Since the X-band tracking system of IKAROS is same as the one of Hayabusa spacecraft, this process noise assumption is determined by the heritage of Hayabusa operation [8]. Three cases are calculated with different tracking arc and attitude conditions. The tracking data set are provided using 4 or 6 sets of 3 days tracking data without maneuvers. Those conditions are summarized in Tab. 1. The values of the coefficients $\overline{C}_n$ are assumed as (3.17E-01, 2.05E-05, 7.90E-02, 3.17E-04, 6.53E-01), which considers the deformation of spinning solar sail. The solar sail area is assumed as 175 m^2. The solar sail deformation model is developed by Tsuda [9].

Table 1. Tracking data conditions for covariance analysis

Case	Tracking arc [days]	Solar cone angle [deg]
1	47	20 to 48
2	48	40 to 48
3	78	20 to 48

The standard deviation of the spinning solar sail model coefficients are summarized in Fig. 5. The coefficients No. n corresponds to $\overline{C}_n$ which are described in previous section. Comparison between case 1 and 2 implies the impact of attitude condition to the GSM estimation. Absorbing and specular reflecting effect $(\overline{C}_1, \overline{C}_3, \overline{C}_5)$ are derived precisely in case 1, and diffusive reflecting effect $(\overline{C}_2, \overline{C}_4)$ are derived precisely in Case 3. These results describes that the coefficients $(\overline{C}_2, \overline{C}_4)$ could not detect as a valuable number because the standard deviation is larger than the value itself. Although the coefficients $(\overline{C}_2, \overline{C}_4)$ strongly depends on the deformation of the sail, those value could be considered if the deformation is larger than we expected.

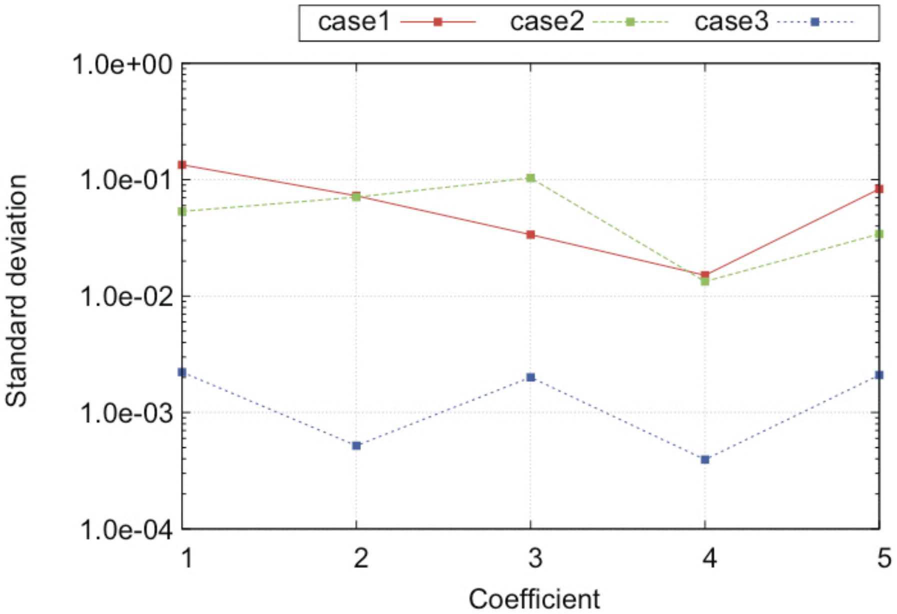

Figure. 5 Standard deviation of the spinning solar sail model parameter

The covariance analysis for different size of the solar sail is investigated to understand the parameter estimation for future solar sail exploration. The trajectory condition is the same as Case 3 of Tab. 1. Three sizes of spinning solar sails are analyzed (ϕ 20 m, 50 m, 100 m). The coefficients of spinning solar sail model $\overline{C}_n$ are the same. Figure 6 describes the standard deviation of the spinning solar sail coefficients. The standard deviations of the coefficients are smaller when the solar sail size becomes larger. These results indicate that the coefficients of deformation $\left(\overline{C}_2,\overline{C}_4\right)$ become more important if the solar sail size becomes larger. The size of the IKAROS solar sail is about 200 m^2, which is small enough to ignore the deformation effect for the solar sail force modeling.

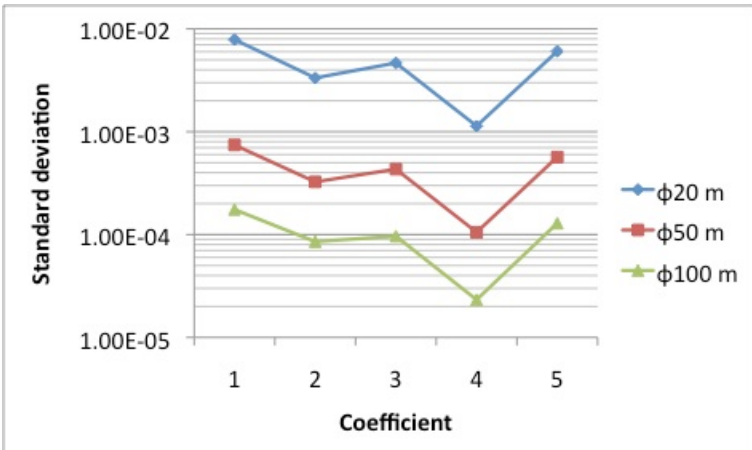

Figure. 6 Standard deviation of the spinning solar sail model parameter with respect to the sail's size

4. Solar Sail Force Estimation using Real Tracking Data

This section investigates the solar sail force modeling for IKAROS using real tracking data. The IKAROS spacecraft deployed the solar sail successfully on June 9th, and it continues collecting the tracking data on the transfer trajectory to the Venus (Fig. 7). The deployment condition of the solar sail was also confirmed by the deployable camera. X/X band Doppler observable is obtained during every operation day. In terms of solar sail force parameter estimation, the tracking data with maneuver is not preferable because the solar sail force submerges in those maneuvers. In this study, nine coasting arcs are investigated, and summarized in Tab. 2. Each arc has continuous tracking data without the attitude control maneuver. Table 2 also summarized the solar cone angle and the Earth angle. Those angles are the angle between the spin axis and the Sun and the Earth direction, respectively. The solar cone angle of the IKAROS is strongly restricted by the power requirement. The Earth angle is also restricted by the location of the antenna on the IKAROS spacecraft. IKAROS has two low gain antennas (LGA) and each of the antenna points along the spin axis. Therefore, IKAROS cannot communicate with the Earth if the Earth angle is around 90 deg.

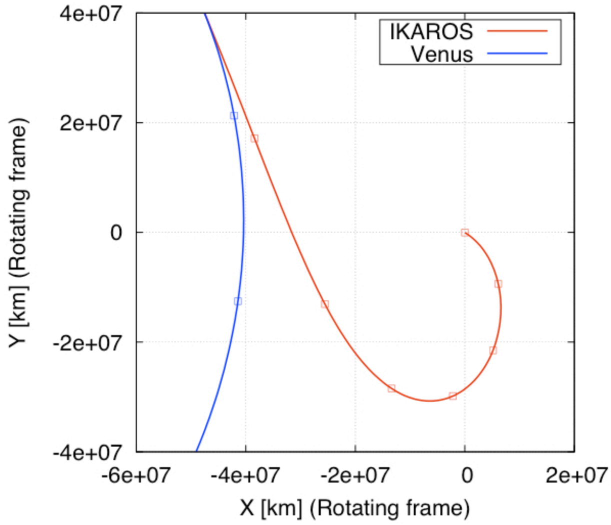

Figure. 7 Interplanetary Trajectory of IKAROS spacecraft (Earth center, Earth-Sun fixed rotating frame)

Table 2. Coasting arcs of IKAROS operation

Arc no.	Tracking date	Solar cone angle [deg]	Earth angle [deg]
1	2010/6/10-2010/6/14	12.5	47.8
2	2010/6/21-2010/6/26	15.4	43.0
3	2010/7/2-2010/7/7	12.1	48.7
4	2010/8/26-2010/8/30	26.4	61.1
5	2010/9/4-2010/9/8	29.2	67.9
6	2010/9/9-2010/9/14	29.9	76.2
7	2010/9/28-2010/10/3	22.9	121.2
8	2010/10/3-2010/10/6	17.9	130.4
9	2010/10/12-2010/10/18	7.6	141.2

In this analysis, the overlap comparison of solar sail acceleration is investigated to evaluate the solar sail force estimation. Table 3 summarizes the tracking data set and solar sail force models for this analysis. Each case overlaps some the tracking arc to compare the estimated solar sail acceleration. Single plane model is used for single arc estimation and spinning solar sail model is used for multiple arcs estimation. In all cases, state vector and solar sail model parameter is estimated. Also un-modeled small force is estimated for each arc, though the value is relatively small (about 1 % of the entire solar radiation pressure). In case of single plane force model, the reflectivity and the area are estimated as global parameters. The three parameters $\left(\overline{C}_1,\overline{C}_3,\overline{C}_5\right)$ are estimated as global parameters in case of spinning solar sail model. The solar sail model parameters are selected by the result of the covariance analysis that discuss at the previous section. The Earth orientation model for terrestrial to celestial coordinate transformation is compliant with IAU 2000A CIO based. JPL ephemeris DE423 is used to calculate the planetary perturbations.

Table 3. Tracking data set for solar sail parameter estimation

Case	Tracking data arc no.	Solar sail force model
1	1	Single plane solar sail model
2	1, 2	Spinning solar sail model
3	1, 2, 3	Spinning solar sail model
4	4	Single plane solar sail model
5	4, 5	Spinning solar sail model
6	4, 5, 6	Spinning solar sail model
7	7	Single plane solar sail model
8	7, 8	Spinning solar sail model
9	7, 8, 9	Spinning solar sail model

The residuals of case 6 and 9 are described in Fig. 8 and 9, respectively. The residuals of case 6 are larger than the residuals of case 9 because the Earth angle is near to 90 deg. Because of the LGA location, the gain of the LGA becomes smaller and the noise becomes larger in this arcs. Some of the pass has large variation than the others because of the weather condition of the ground station.

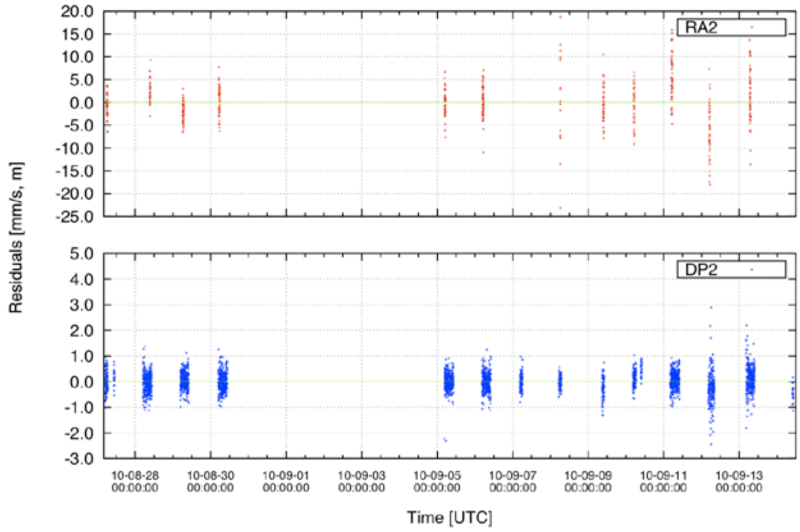

Figure. 8 2-way Doppler and range residuals of case 6

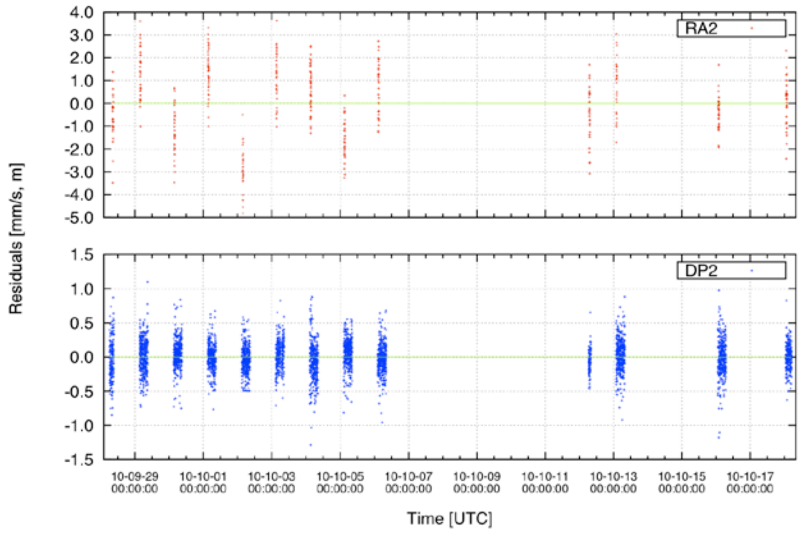

Figure. 9 2-way Doppler and range residuals of case 9

The overlap comparisons of the estimated solar sail acceleration are described in Fig. 10, 11 and 12. Each figure compares the acceleration in radial, transverse and normal components (RTN). The R axis points from the Sun along the radius vector toward the spacecraft. The N axis is normal to the orbital plane. The solar sail acceleration between case 1, 2 and 3 are compared in arc 1, and describes in Fig. 10. The difference of the acceleration is about 1 % of the solar sail acceleration. The largest component is the normal component in this comparison. Figure 11 shows the comparison between case 4, 5 and 6 in arc 4. The difference of the acceleration is about 30 % of the solar sail acceleration. Since the Earth angle of this tracking arcs are close to 90 deg, the quality of the radiometric tracking data are relatively poor. Therefore the estimated solar sail acceleration also varies with respect to the data selection. The comparison of case 7, 8 and 9 is illustrated in Fig. 12. The difference is about 3 % of solar sail acceleration. The difference is larger than Figure 10 because the Earth distance of the comparison arcs is larger. Since case 9 includes the variety of solar cone angle in its tracking arcs, the covariance of the estimated parameters are smaller than case 3. However, the acceleration difference of the Fig. 12 is larger than Fig. 10 in this comparison. This difference could be caused by the attitude determination error in the arc 7, 8 and 9. The attitude of IKAROS is determined by the sun sensor and the Doppler shift due to the antenna offset from the spin axis. Therefore, the precision of the attitude determination strongly depends on the displacement of antenna. The LGA was switched between the arc 6 and 7, and this could make error on the attitude.

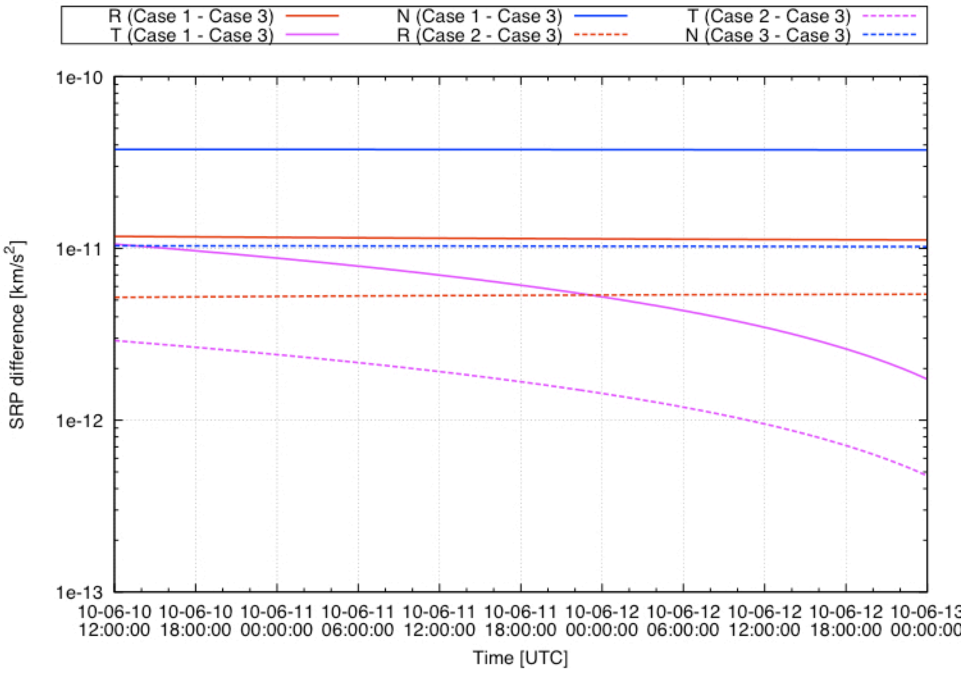

Figure. 10 Comparison of estimated SRP acceleration (arc 1, case 1, 2, 3)

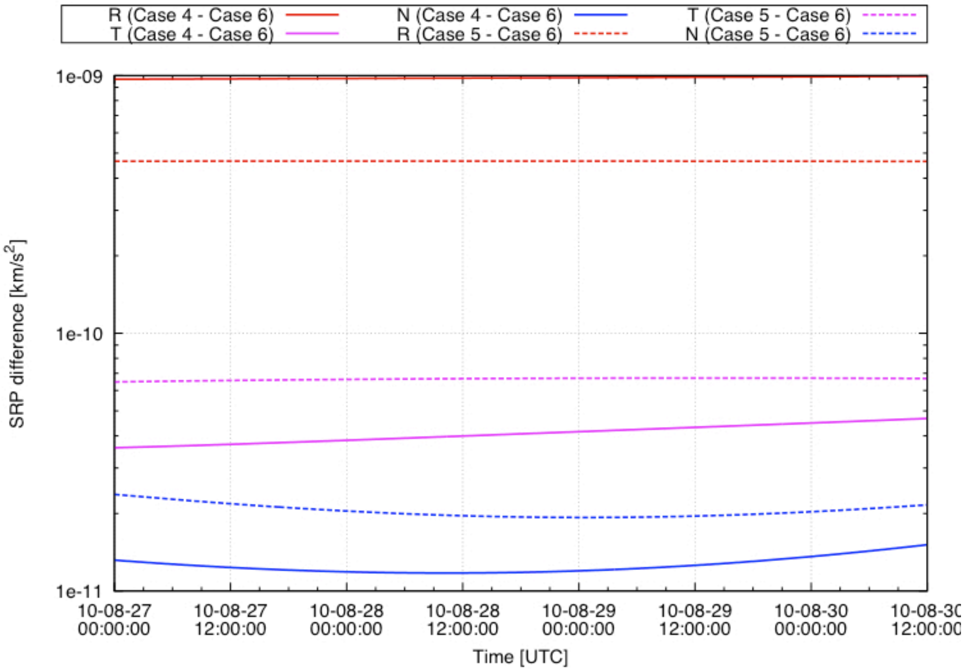

Figure. 11 Comparison of estimated SRP acceleration (arc 4, case 4, 5, 6)

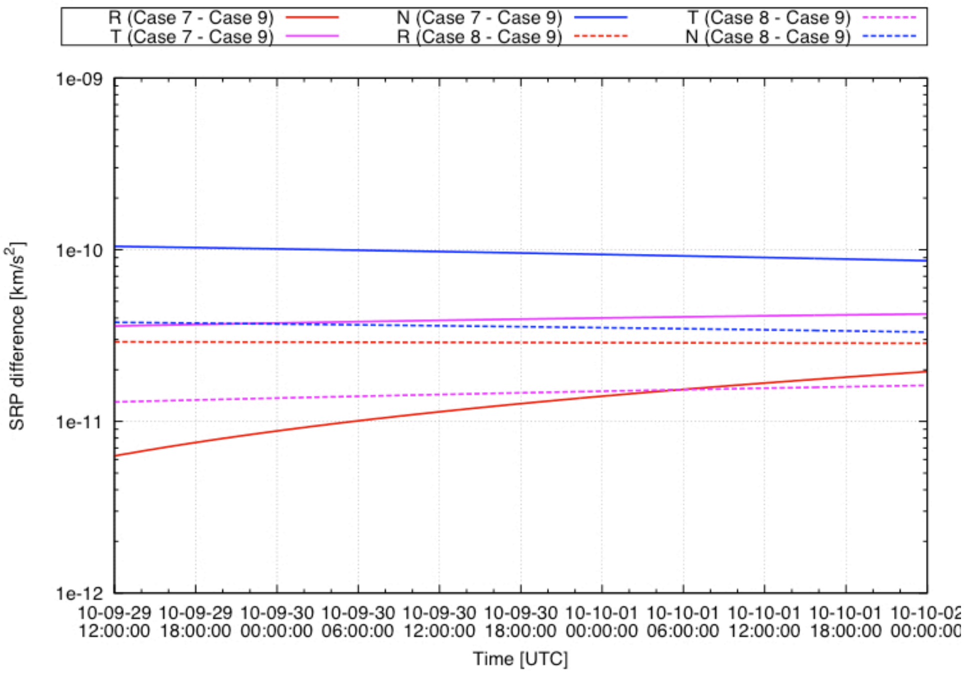

Figure. 12 Comparison of estimated SRP acceleration (arc 7, case 7, 8, 9)

5. Conclusion

The solar sail force modeling for a spinning solar sail spacecraft was investigated considering the deformation. The solar sail force model specialized for the spinning solar sail was presented including the arbitrary deformation of the sail. Five parameters are required to define the spinning solar sail force.

The covariance analysis for the IKAROS spacecraft using the spinning solar sail model were investigated to find the ability of solar sail modeling along the IKAROS mission sequence. It is found that two of the spinning solar sail parameter is hard to estimate as a valuable number.

The estimated solar sail acceleration is evaluated by the overlap comparison using the IKAROS tracking data of the coasting arcs. The solar sail acceleration is estimated within 3 % accuracy in normal Earth angle. The estimation results strongly depend on the quality of the tracking data and the attitude data.

6. Acknowledgements

The authors are deeply grateful to Dr. S. Ishibashi and Mr. S. Taniguchi in Fujitsu Ltd for fruitful discussion on the orbit determination of IKAROS and providing the tracking data.

7. References

[1] Leipold, M., Seboldt, W., Lingner, S., Borg, E., Herrmann, A., Pabsch, A., Wagner, O., and Brueckner, J., "Mercury sun-synchronous polar orbiter with a solar sail", ACTA ASTRONAUTICA, Vol. 39, 143 – 151, 1996.

[2] Morrow, E., Scheeres, D. J., and Lubin, D., "Solar sail orbit operations at asteroids", JOURNAL OF SPACECRAFT AND ROCKETS, Vol. 38, 279–286, 2001.

[3] Dachwald, B., "Optimal solar-sail trajectories for missions to the outer solar system", JOURNAL OF GUIDANCE, CONTROL, AND DYNAMICS, Vol. 28, 1187-1193, 2005.

[4] Reichhardt, T., "Setting sail for history", NATURE, Vol. 433, 678-679, 2005.

[5] Tsuda, T., Mori, O., Sawada, H., Yamamoto, T., Saiki, T., Endo, T. and Kawaguchi, J., "Flight Status of IKAROS Deep Space Solar Sail Demonstrator", Proceedings 61st International Astronautical Congress, Prague, CZ, 2010.

[6] Montenbruck, O. and Gill, E.: "Satellite Orbits: Models, Methods and Applications", Springer, 2005.

[7] Rios-Reyes, L. and Scheeres, D. J., "Generalized model for solar sails", JOURNAL OF SPACECRAFT AND ROCKETS, Vol. 42, 182-185, 2005.

[8] Ikeda, H., Kominato, T., Matsuoka, M., Ohnishi, T. and Yoshikawa, M., "Orbit analysis of hayabusa around asteroid Itokawa", Proceedings 57th International Astronautical Congress, 2006.

[9] Tsuda, Y., "Stability Criteria for the Spinning Spacecraft with Large Flexible Membrane", AIAA Guidance, Navigation and Control Conference and Exhibit, Honolulu, Hawai, 2008.